Human Molecular Genetics, 2014, Vol. 23, No. 21 **5781–5792**
doi:10.1093/hmg/ddu296
Advance Access published on June 11, 2014

POMK mutations disrupt muscle development leading to a spectrum of neuromuscular presentations

Stefania Di Costanzo[1,2], Anuradha Balasubramanian[3], Heather L. Pond[1,2], Anete Rozkalne[3], Chiara Pantaleoni[6], Simona Saredi[6], Vandana A. Gupta[3], Christine M. Sunu[3], Timothy W. Yu[3], Peter B. Kang[4], Mustafa A. Salih[7], Marina Mora[6], Emanuela Gussoni[3], Christopher A. Walsh[3,5,*] and M. Chiara Manzini[1,2,*]

[1]Department of Pharmacology and Physiology and [2]Integrative Systems Biology, The George Washington University School of Medicine and Health Sciences, Washington, DC 20037, USA, [3]Division of Genetics and Genomics and the Manton Center for Orphan Disease Research, [4]Department of Neurology, [5]Howard Hughes Medical Institute, Boston Children's Hospital, Boston, MA 02115, USA, [6]Division of Neuromuscular Disease and Neuroimmunology, Fondazione di Ricovero e Cura a Carattere Scientifico Istituto Neurologico C. Besta, 20126 Milan, Italy and [7]Division of Pediatric Neurology, Department of Pediatrics, King Saud University College of Medicine, Riyadh 11461, Saudi Arabia

Received February 18, 2014; Revised May 16, 2014; Accepted June 9, 2014

Dystroglycan is a transmembrane glycoprotein whose interactions with the extracellular matrix (ECM) are necessary for normal muscle and brain development, and disruptions of its function lead to dystroglycanopathies, a group of congenital muscular dystrophies showing extreme genetic and clinical heterogeneity. Specific glycans bound to the extracellular portion of dystroglycan, α-dystroglycan, mediate ECM interactions and most known dystroglycanopathy genes encode glycosyltransferases involved in glycan synthesis. *POMK*, which was found mutated in two dystroglycanopathy cases, is instead involved in a glycan phosphorylation reaction critical for ECM binding, but little is known about the clinical presentation of *POMK* mutations or of the function of this protein in the muscle. Here, we describe two families carrying different truncating alleles, both removing the kinase domain in POMK, with different clinical manifestations ranging from Walker–Warburg syndrome, the most severe form of dystroglycanopathy, to limb-girdle muscular dystrophy with cognitive defects. We explored POMK expression in fetal and adult human muscle and identified widespread expression primarily during fetal development in myocytes and interstitial cells suggesting a role for this protein during early muscle differentiation. Analysis of loss of function in the zebrafish embryo and larva showed that *pomk* function is necessary for normal muscle development, leading to locomotor dysfuction in the embryo and signs of muscular dystrophy in the larva. In summary, we defined diverse clinical presentations following *POMK* mutations and showed that this gene is necessary for early muscle development.

INTRODUCTION

Dystroglycanopathies are a group of muscle disorders that are often associated with brain and ocular defects, and they display great genetic and clinical variability (1,2). Phenotypic presentations can vary widely, from Walker–Warburg syndrome (WWS) (MIM 236670), a perinatal lethal form of congenital muscular dystrophy (CMD) also characterized by severe cortical and ocular malformations (3,4), to milder postnatal neuromuscular phenotypes with no brain malformations,

*To whom correspondence should be addressed at: Department of Pharmacology and Physiology, The George Washington University School of Medicine and Health Sciences, 2300 Eye Street NW, Ross Hall 650, Washington, DC 20037, USA. Email: cmanzini@gwu.edu (M.C.M.); Division of Genetics and Genomics, Boston Children's Hospital, Howard Hughes Medical Institute, Harvard Medical School, Room 15062.2, Center for Life Sciences Building, 3 Blackfan Circle, Boston, MA 02115, USA. Email: christopher.walsh@childrens.harvard.edu (C.A.W.)

© *The Author 2014. Published by Oxford University Press. All rights reserved.*
For Permissions, please email: journals.permissions@oup.com

such as CMD associated with intellectual disability or limb-girdle muscular dystrophy (LGMD), a type of MD primarily affecting the proximal muscles (MIM253600; 607155) (5,6).

Sixteen different genes have been found mutated in dystroglycanopathies and have identified glycosylation of dystroglycan as the primary molecular mechanism disrupted in the affected tissues (2,7). Dystroglycan is a transmembrane glycoprotein, which acts as the link between the dystrophin complex inside the cell and extracellular matrix (ECM) components such as laminin on the outside (8). In tissues where the ECM in the basement membrane controls development and maintenance such as the muscle and kidney, dystroglycan-mediated interactions are necessary for tissue integrity and function and disruptions lead to muscular dystrophy and renal malformations. In addition, the lamination of multiple neuronal epithelia in the retina, cerebral cortex and cerebellum is disorganized in many dystroglycanopathy cases, identifying an important role for dystroglycan in neuronal proliferation and migration (9,10).

Only a handful of patients carry mutations in the *dystroglycan* (*DAG1*) gene itself (MIM 128239), and nine of the known dystroglycanopathy genes are confirmed or predicted glycosyltransferases involved in assembling specific glycans on the mucin domain of the extracellular portion of the protein, α-dystroglycan (α-DG) (2). Each glycosyltransferase catalyzes a very specific reaction and the study of these proteins has revealed a complex pattern of glycosylation controlling interactions between α-DG and the ECM. Analyses via mass spectrometry have identified a variety of glycan species on α-DG (11,12), but one of the most important portions of the laminin-binding site appears to be a trisaccharide core composed of *N*-acetylgalactosamine, *N*-acetylglucosamine and mannose (Man), and designated as core M3 (13). *Protein O-mannosyltransferases 1 and 2* [*POMT1* (MIM 607423) and *POMT2* (MIM 607439)], which were some of first genes found to be mutated in dystroglycanopathies (14,15), catalyze the initiation of O-linked chains starting with the Man residue. Two additional glycosyltransferases, *GTDC2* (MIM 614828) and *B3GALNT2* (MIM 610194), add the GlcNac and GalNac, respectively (16–18). Loss-of-function mutations in these three genes cause WWS and severe eye–brain–muscle phenotypes confirming the critical role of the core M3 glycan in dystroglycan function.

However, laminin binding is also regulated by phosphorylation of the Man residue in the core M3 glycan (13), and a protein involved in this phosphorylation event has been recently identified as the putative Sugen Kinase 196, *SGK196* (MIM 615247), also called protein O-mannose kinase or *POMK* (18). Missense mutations in *POMK* have been described in one WWS case as part of a screen for genes that affect α-DG glycosylation (7) and recently in a family with a phenotype similar to merosin-deficient muscular dystrophy (19). However, little is known about the clinical presentation of patients carrying *POMK* mutations and the role of this gene during fetal development.

Here we present two families carrying loss-of-function *POMK* mutations but displaying variable presentations ranging from WWS to LGMD indicating that loss of POMK activity differentially affects dystroglycan function. We show that *POMK* protein and mRNA are highly expressed in muscle and brain tissues during human fetal development and in particular during myocyte differentiation. In developing zebrafish embryo, *pomk* knockdown rapidly leads to decreased mobility in the chorion and to the development of muscular dystrophy by 3 days postfertilization (dpf), indicating that function of this protein is important during early muscle development.

RESULTS

Identification of POMK mutations in LGMD and WWS

Family 1 presented with LGMD and cognitive impairment (Table 1), a phenotype at the milder end of the dystroglycanopathy spectrum. Two affected siblings were born to a Jordanian first cousin union residing in Saudi Arabia (Fig. 1A, Family 1).

Table 1 Clinical presentation of affected individuals.

	Family 1 Patient 1	Family 1 Patient 2	Family 2 Patient 3
Mutation	c.325C > T, p.Q109*	c.325C > T, p.Q109*	c.286delT, p.F96fs c.905T > A, p.V302D
Age	25	13	Deceased at 4 years
Gender	F	M	M
Age of onset	Infancy	Infancy	Infancy
First presentation	Floppiness and delayed walking at 18 months	Floppiness and delayed walking at 18 months	Brain malformation upon fetal brain MRI at 32 weeks
Muscle findings			
Diagnosis	LGMD	LGMD	CMD
Ambulation	Still ambulant, climbs stairs using banister	Still ambulant, detectable defect in posture and gait	Spontaneous motility absent at 7 months
Creatine kinase	1090 (22 years)	1420 (9 years)	3985 (7 months)
Muscle biopsy	n/a	Dystrophic, positive for all markers tested	Absence of muscle fibers
EMG	n/a	Myopathic	n/a
Brain findings			
Brain imaging	Temporal lobe arachnoid cyst	Mega cisterna magna	Cobblestone lissencephaly and hydrocephalus
Seizures	No	No	Tonic seizures starting at 7 months
IQ testing	80 (20 years)	83 (7.5 years)	Severe impairment
Ocular findings			
Eye exam	Normal	Normal	Right eye glaucoma, bilateral retinal degeneration

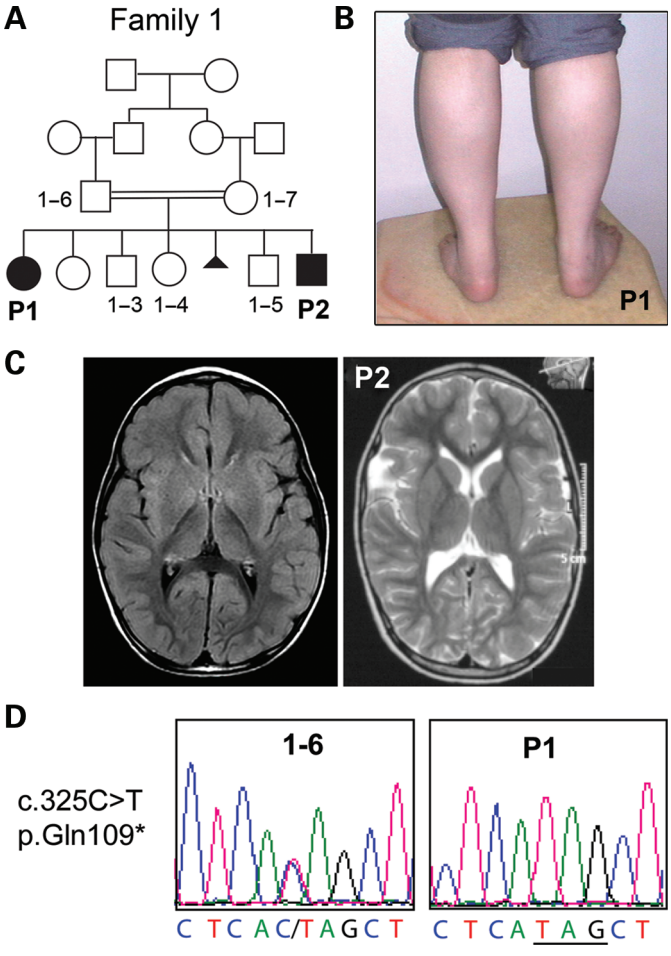

Figure 1. A nonsense mutation in POMK causes LGMD and cognitive deficits. (**A**) Two affected individuals, a female (P1) and a male (P2), were born to consanguineous parents (1–6 and 1–7) in Family 1. DNA was collected from all numbered individuals. Calf hypertrophy was observed in P1 (**B**) and P2 (Supplementary Material, Fig.S1B), and an arachnoid cyst was also identified on the left hemisphere in P2 via MRI imaging (**C**). (**D**) Both individuals carried a nonsense mutation truncating the POMK protein at glutamine 109 (c.325C>T). Parents were confirmed to be heterozygous for the variant.

Patient 1 is a female who is currently 25 years of age and first presented in infancy with weakness and delayed motor development, learning to walk at 18 months. In her latest neurological exam at age 22, she displayed increased proximal weakness, calf pseudohypertrophy (Fig. 1B), hyporeflexia, mild facial weakness and Gower's sign. Creatine kinase (CK) levels were elevated to 1090 U/l compared with normal levels <140. At the time of the last follow-up visit, she was still ambulatory, but needed to hold on to the banister to climb stairs. Her IQ was tested at 80, which is in the low average range, but she required special schooling and was diagnosed as intellectually disabled. A CT scan revealed an enlargement of the cisterna magna, but overall normal brain structure and gyration pattern (Supplementary Material, Fig. S1A).

The youngest brother in the family, Patient 2, had a similar presentation in infancy. He was 7.5 years old at the time of his last neurological exam and was more mildly affected (Table 1; Supplementary Material, Fig. S1B). He is now 13 years old and can still climb stairs without support, though his posture and gait are affected by the muscle weakness. CK levels were last measured at 9 years of age at 1420 U/l. A muscle biopsy was performed, and while showing signs of cell death and regeneration typical of muscular dystrophy, muscle fibers were reported positive for all markers tested (dystrophin, utrophin, merosin, dysferlin, α-, β-, γ- and δ-sarcoglycans and β-dystroglycan). At the time of testing, dystroglycanopathy was not yet considered as part of the differential diagnosis and α-dystroglycan glycosylation levels were not assayed. Patient 2 also requires special schooling and his IQ is 83. MRI imaging showed an arachnoid cyst by the left temporal lobe, but an otherwise normal brain (Fig. 1C). Arachnoid cysts are non-specific findings (20) and are not usually associated with LGMD, so it is unclear whether they share the same genetic cause in these cases.

Due to the consanguinity in the family, we expected the disease-causing mutation to be harbored in a region of homozygosity shared by all affected individuals (21). Total genomic DNA was hybridized to Illumina Human610-Quad for genome-wide genotyping and homozygosity mapping was performed using algorithms designed in house. Loci for all known LGMD and dystroglycanopathy genes were excluded. Three regions of homozygosity were identified: the largest one spanned the centromere of chromosome 8 (chr 8p12-q12 from rs11773958 to rs10108135) and extended for 25.5 Mb containing 106 genes, the other two regions were smaller, 2.6 Mb on chr18p11 (rs1466421–rs2864780) and 0.6 Mb on chr6q25 (rs9365059–rs598558), and contained 12 and 8 genes, respectively (Supplementary Material, Fig. S1C). All 126 genes were sequenced in Patient 1 using a targeted next-generation sequencing approach on an Illumina HiSeq machine following capture on a NimbleGen custom array. 92.5% of bases in the regions were covered at 5× and only two homozygous variants leading to protein sequence changes were identified in the largest region on chromosome 8: a stop codon in *POMK* (c.325C > T, p.Gln109*, Fig. 1D) and a missense change in *GPR124* (c.1124C > A, p.Thr375Lys). Both variants were confirmed by Sanger sequencing and were present in homozygosity in the affected individuals and in heterozygosity in the parents. Neither variant was present in 6500 exomes in the Exome Variant Server from the NHLBI Exome Sequencing Project or in 831 exomes sequenced in the Walsh lab and including Middle Eastern controls (22), showing that these changes are extremely rare. *GPR124* is a G protein-coupled receptor, which is part of the adhesion-GPCR family, and extensive analysis in mouse models lacking this gene revealed an essential role in vascular development which is not consistent with the patients' phenotype (23,24). *POMK* is predicted to encode a 350 amino acid single-pass transmembrane protein containing a protein kinase-like domain, which is mostly removed by the p.Gln109* mutation (Fig. 2E). We sequenced *POMK* in a cohort of 57 cases in the LGMD and mild dystroglycanopathy spectrum, but did not identify additional mutations.

We then queried a database of 28 exomes generated from cases with more severe dystroglycanopathy presentations and identified one additional individual with mutations in *POMK*. Patient 3 was a male born from non-consanguineous Italian parents (Fig. 2A) and he presented with the most severe form of dystroglycanopathy, WWS (Table 1). Macrocephaly and hydrocephalus were diagnosed *in utero* upon prenatal ultrasound at 32 weeks of gestation and delivery via cesarean section was

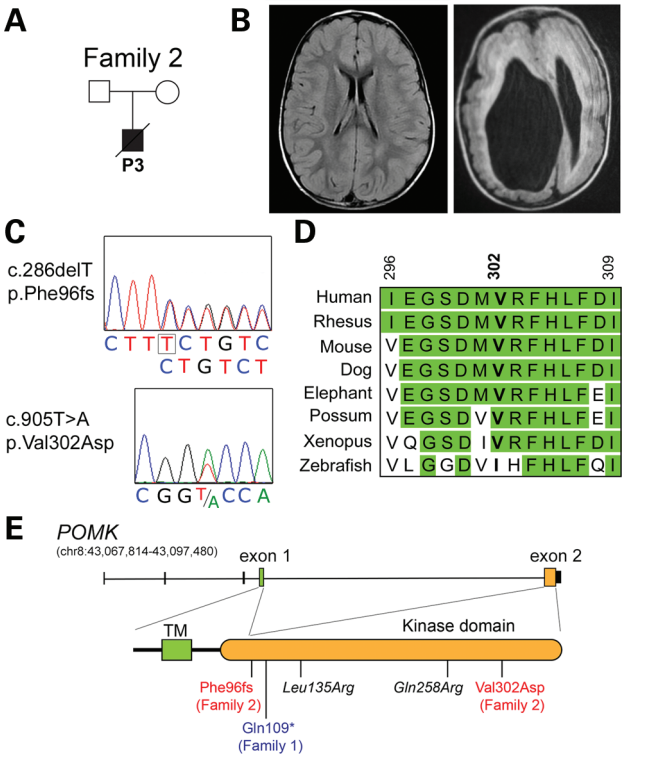

Figure 2. Severe compound heterozygous changes in POMK cause WWS. (**A**) Family 2 was an Italian trio including a boy affected by WWS (P3). (**B**) One of the diagnostic features of WWS, cobblestone lissencephaly with hydrocephalus, was noted upon MRI imaging. (**C**) Exome sequencing identified two heterozygous mutations in POMK, which were confirmed by Sanger sequencing. One change was a 1 bp deletion leading to a frameshift (c.286delT) and the second change was a missense affecting a highly conserved amino acid (c.905T > A) (**D**). (**E**) The truncating mutations in Families 1 and 2 are found very early in the protein and are both predicted to completely remove the putative kinase domain in POMK.

performed at 34 weeks. Head circumference was large (38 cm; >97th percentile) and a ventriculoperitoneal shunt was inserted because of substantial intracranial hypertension. Hypotonia, glaucoma of the right eye and bilateral retinal degeneration plus severe bilateral sensorineural hearing loss were noted. Following severely delayed psychomotor development and tonic seizures, additional testing was performed at 7 months of age. CK was 3985 U/l and muscle fibers were reported absent upon muscle biopsy. Radiological imaging via MRI showed cobblestone lissencephaly, agenesis of the corpus and severe cerebellar vermis hypoplasia (Fig. 2B). Electroencephalography revealed poor organization of background activity and multifocal epileptic abnormalities. He had two compound heterozygous variants in *POMK*: a frameshift change (c.286delT, p.Phe96Phefs*19) and a missense change (c.905T > A, p.Val302Asp) in a highly conserved amino acid predicted to be damaging by two independent pathogenicity prediction softwares (SIFT = 0 with 0 being the most damaging; Polyphen2 = 0.98 with 1 being the most damaging) (Fig. 2C and D). These changes were not present in any of the databases listed above.

Another patient reported to have a typical WWS presentation was described by Jae *et al*. (7), carrying compound heterozygous missense variants in *POMK* (Fig. 2E), and the same p.Gln109* mutation was recently identified in a Lebanese family with CMD, hypomyelination and intellectual disability (19). Our findings expand the phenotypic variation in *POMK* mutations despite the fact that both patients presented here carry severe protein-truncating mutations.

POMK is highly expressed in the brain and muscle during development

To define the expression pattern of *POMK* during human development, we used quantitative PCR (qPCR) to study relative expression levels of *POMK* expression in a panel of human tissues (Fig. 3A). The highest expression in both fetal and adult tissues was observed in the brain, skeletal muscle, kidney and heart, which are usually the most severely affected tissues in the patients and is consistent with expression patterns observed for other dystroglycanopathy genes (16). Analysis across different regions in the adult human brain also showed highest expression in the cerebral cortex (Fig. 3B). Given the high mRNA expression of *POMK* in the cerebral cortex, we asked whether expression in the brain was dynamic. We used mouse cerebral cortex samples collected throughout embryonic and postnatal development up to weaning for western blot analysis and found that Pomk was expressed as early as embryonic day (E) 12, but noted marked increase in Pomk expression starting from the later stages of embryonic development at E16 (Fig. 3C).

Expression levels were comparable in the brain, kidney and heart in both time-points tested via qPCR, but skeletal muscle levels were reduced by >60% in the adult. We then tested POMK expression in the fetal and adult muscle by immunohistochemistry and observed a consistent result. In human fetal muscle samples, co-localization of POMK with laminin shows the expression of POMK around nuclei located within the laminin staining on the surface of myofibers (Fig. 3D,i). In addition, interstitial cells strongly positive for POMK were also detected outside of laminin staining (Fig. 3D,ii). Co-localization of POMK with anti-human lamin A/C in human fetal muscle revealed POMK reactivity distributed at the outer edge of the nuclear envelope, suggesting a possible localization in the Golgi apparatus and endoplasmic reticulum (Fig. 3E). In adult muscle, co-localization of POMK and laminin revealed the presence of interstitial cells strongly positive for POMK expression (Fig. 3F,i). In addition, cells located within blood vessels also expressed POMK (Fig. 3F,ii). Co-staining of POMK with lamin A/C in adult human muscle revealed again the presence in interstitial cells positive for both markers and occasional intramyofiber cytoplasmic reactivity (not shown). This dynamic expression pattern of POMK in the human muscle suggests a possible important role during early development as POMK appears to be ubiquitously expressed in myocytes and interstitial cells, but then expression decreases and becomes restricted to a small interstitial population between myofibers or cells associated with blood vessels.

Silencing of POMK in differentiating human fetal muscle cells leads to reduction in dystroglycan glycosylation

To better understand the role of POMK during muscle differentiation, human fetal myogenic cells were purified based on the expression of the melanoma cell adhesion molecule, MCAM

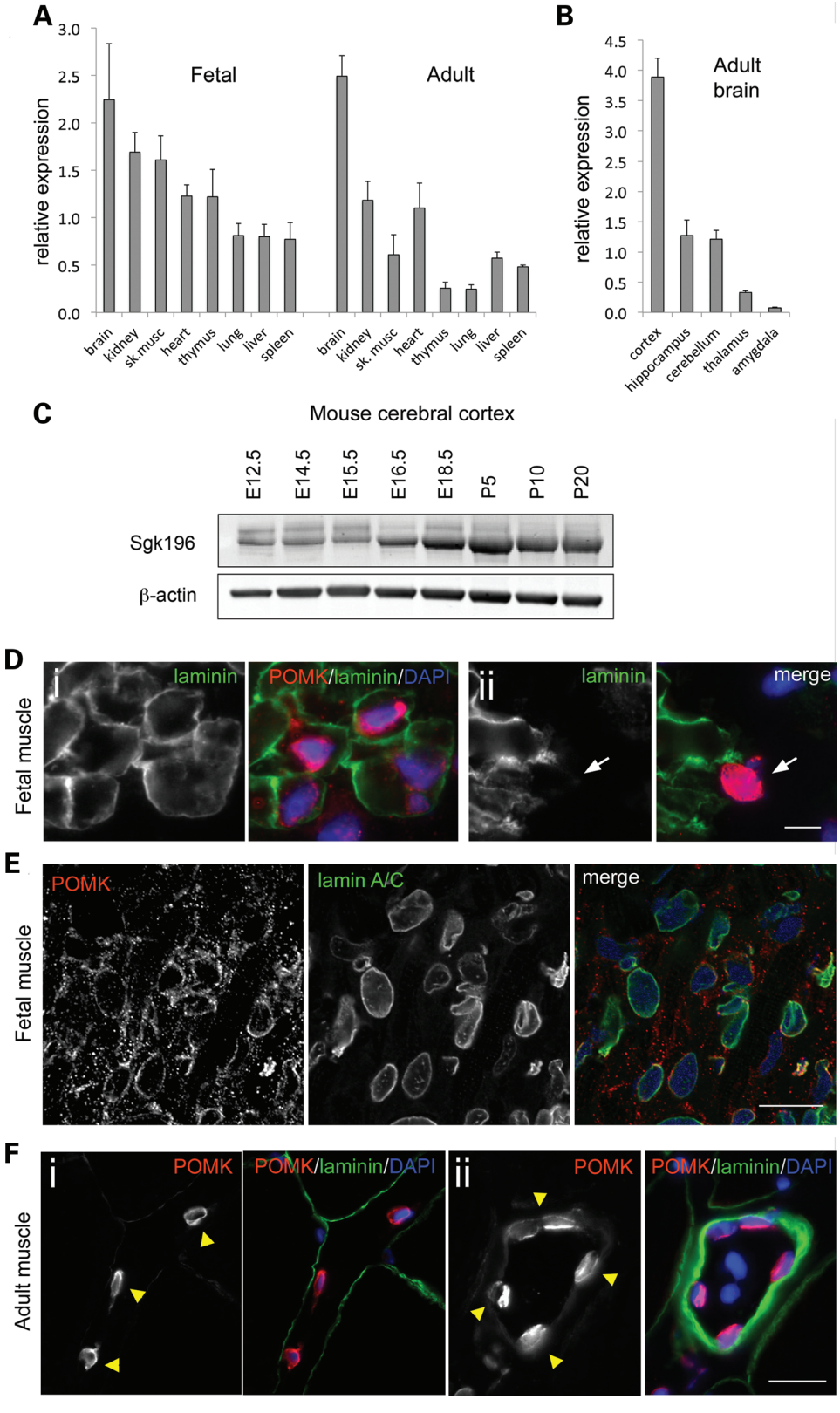

Figure 3. POMK is highly expressed during muscle and brain development. (**A** and **B**) Quantitative PCR analysis of POMK expression in human tissues shows highest expression in brain, skeletal muscle, kidney and heart in fetal and adult tissues. Highest expression in the brain is observed in the cerebral cortex. (**C**) Cortical expression was studied in the mouse and found to be dynamic increasing after E16.5. (**D**) The expression analysis of POMK in the developing human muscle was also revealed to be dynamic. In fetal muscle cells, POMK is found in both laminin-positive (i) and laminin-negative cells (arrow in ii). Scale bar: 10 μm (**E**) Lamin A/C staining outlines the nuclear envelope and POMK decorates perinuclear and cytoplasmic structures in all cells in the fetal muscle. Scale bar: 50 μm (**F**) In the adult human muscle, POMK expression is restricted to interstitial cells between the myofibers and in cells closely associated with the blood vessels (yellow arrowheads). Scale bar: 50 μm.

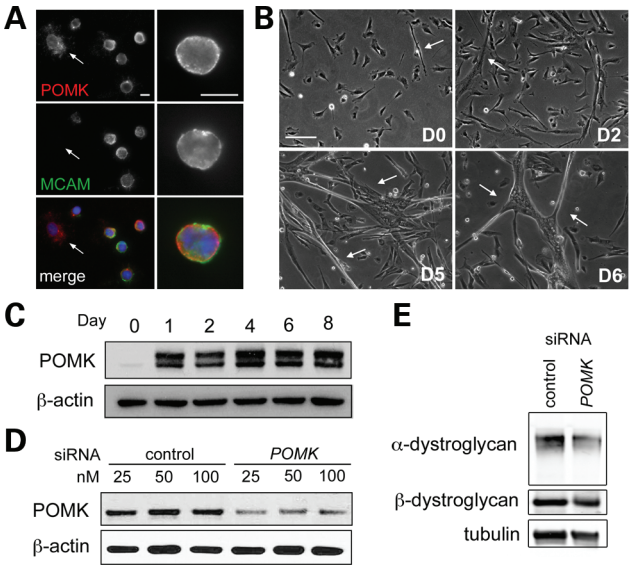

Figure 4. POMK knockdown reduces dystroglycan glycosylation but does not affect myotube formation. (**A**) POMK is highly expressed in both MCAM-positive and MCAM-negative cells (arrow) purified from human fetal muscle. MCAM-positive cells are myogenic cells and we wondered whether POMK knockdown would affect the early stages of myocyte development. Scale bars: 10 μm. (**B**) Purified myocytes will fuse to form myotubes (arrows) over the first week *in vitro*. Scale bar: 100 μm. (**C**) POMK is highly expressed starting at Day 1 after myogenic cell purification. (**D**) A highly efficient siRNA pool was tested and shown to generate consistent knockdown starting at a concentration of 25 nM. (**E**) No effect was observed in myocyte fusion during the first week *in vitro*, but α-DG glycosylation was reduced following POMK knockdown. Day 4 samples are shown.

and differentiated *in vitro* as previously described (25,26). POMK expression was observed in all purified cells including MCAM-positive myogenic cells, indicating that POMK is present in the muscle before differentiation (Fig. 4A). Myogenic cells were induced to differentiate over the course of 8 days: at plating individual cells are evenly distributed around the culture vessel, but between Days 2 and 5 cells begin to elongate and fuse leading to the progressive formation of larger myotubes (Fig. 4B). POMK expression was monitored by western blot on protein lysates harvested at different days following induction of differentiation and we found that it rapidly increased following induction of differentiation and persisted throughout the course of differentiation (Fig. 4C). Interestingly, a protein doublet was observed in differentiating human fetal muscle cells, consistent with the protein doublet seen in embryonic mouse cerebral cortex.

To determine if downregulation of POMK expression in differentiating human muscle cells leads to abnormalities in myotube formation or in the regulation of dystroglycan glycosylation, RNA silencing of *POMK* was induced in mononuclear cells that were then allowed to differentiate *in vitro*. Different concentrations of a pool of small interfering RNA oligonucleotides (siRNAs) designed to reduce POMK expression were tested in parallel with non-targetable (NT) siRNA control, demonstrating that downregulation of POMK expression was effective (Fig. 4D). Myotube formation was monitored in NT- and POMK-silenced cultures, but no significant differences were seen in the overall fusion index between the cultures. In contrast, expression of the glycosylated form of α-DG was significantly decreased in *POMK*-silenced cultures compared with NT-siRNA (Fig. 4E). These findings indicate that while POMK is expressed during the early stages of myocyote differentiation and it regulates α-DG glycosylation, it is not necessary for myocyte fusion and may be involved in later stages of muscle differentiation.

Loss of SGK196 disrupts muscle function and α-DG glycosylation in the zebrafish

To further explore the role of *POMK* loss of function throughout muscle development, we used a protein knock-down approach in the zebrafish embryo. Expression of a gene of interest can be removed by injecting morpholinos oligonucleotides (MOs) targeting either translation initiation or splicing of the mRNA in the fertilized oocyte, and the zebrafish has proven to be a reliable model for human neuromuscular disorders (27). Zebrafish *pomk* (*zgc:101572*) is a two exon gene displaying 59.5% DNA identity to the human gene. We obtained MOs targeted against the start site or the splice donor site in the first intron of the gene and tested both by injection in the fertilized zebrafish embryo at the one- to two-cell stage. Injection at 5 ng revealed comparable results for both MOs, leading to embryos with a small head, delayed ocular development, shortened thicker tail and U-shaped somites at 1 dpf (Fig. 5A). Embryo motility was also reduced in the chorion at this time. Spontaneous locomotor activity is evident in the zebrafish embryo starting at ∼17 hours post-fertilization (hpf) as body coiling movements which often lead to changes in embryo position in the chorion (Fig. 5B; Supplementary Material, Movie 1) (28). These movements are controlled by activation of locomotor programs in the nervous system and responses in the developing muscles in the body. We analyzed *pomk* morphant embryos at 20 hpf and while they displayed a trend towards more frequent coiling in the tail (1.49 ± 0.63 Hz for the morphants compared with 0.44 ± 0.12 Hz for controls; $N = 3$, $P = 0.17$), the tail movement appeared less powerful as the morphants were not able to shift position in the chorion and the head and tail oscillated around the same location (Fig. 5B; Supplementary Material, Movie 2). In fact, while controls performed an average of 0.33 ± 0.09 flips per second where the head could be found to the opposite side of the chorion, the morphants were never observed to move from a fixed position ($N = 3$, $P = 0.006$).

Increased mortality was observed in morphant clutches at the time of hatching between 2 and 3 dpf with a drop from 87.3 ± 5.8% morphant 2 dpf embryos compared with controls to 66.3 ± 11.5% morphant 3 dpf embryos ($N = 5$). At 3 dpf, the tails of surviving morphant larvae were bent (Fig. 5B) and the larvae could not swim normally suggesting muscular weakness. Immunohistochemical analysis of the tail muscle revealed features characteristic of muscular dystrophy. α-DG binds to laminin extracellularly and to dystrophin inside the cell anchoring muscle fibers to the surrounding basement membrane. In the fish muscle, these proteins are concentrated at the regions anchoring the myotomes, the myosepta, which are disrupted in zebrafish models of muscular dystrophy (16,29,30). Laminin and dystrophin expression was reduced in the morphant muscle, as was α-DG glycosylation revealed by VIA4-1 antibody, which recognizes a glycosylated form of the protein.

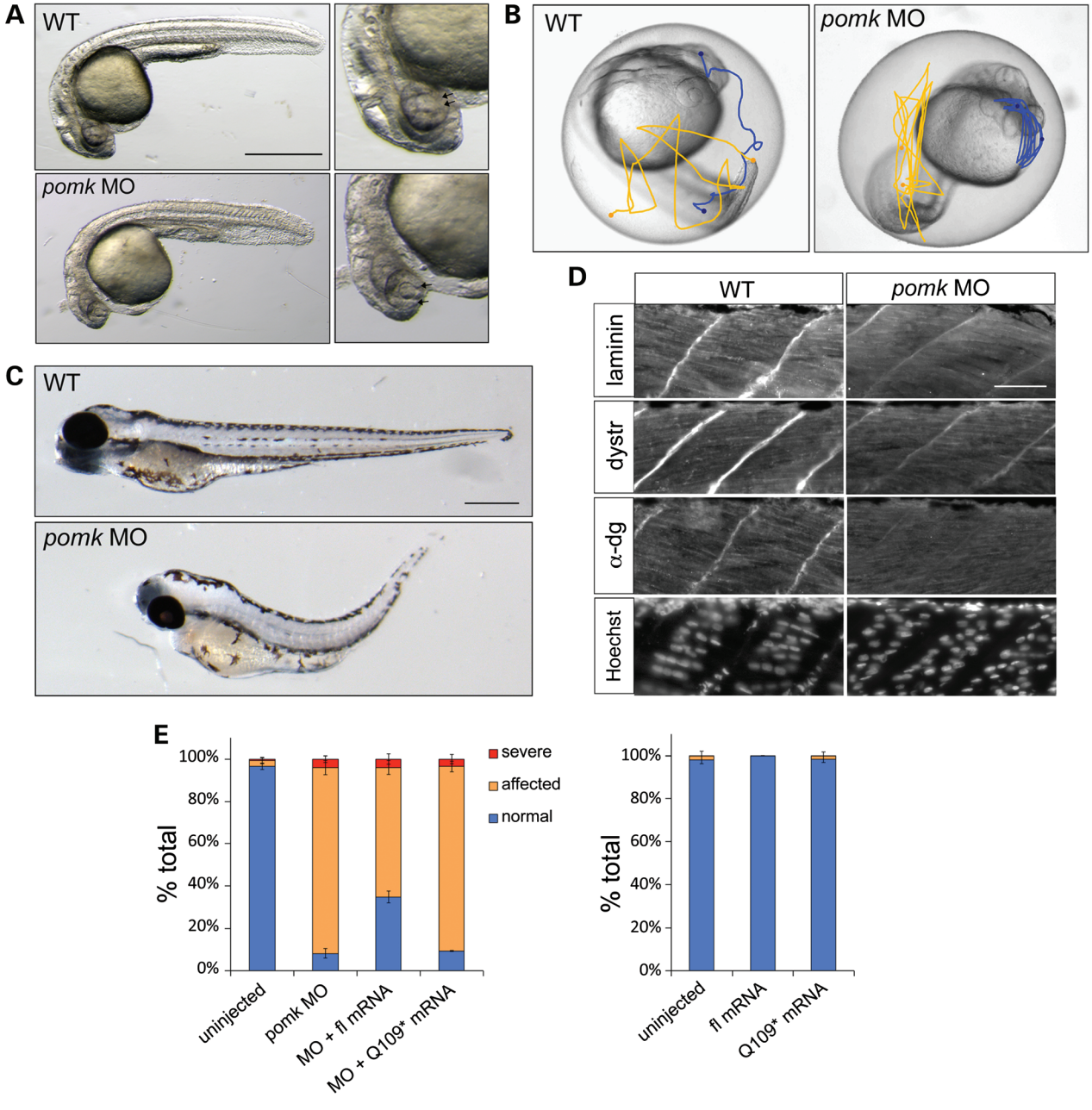

Figure 5. *pomk* knockdown disrupts muscle development in the zebrafish embryo. (**A**) *pomk* MO injection affects brain, eye and muscle development in the zebrafish embryo. The tail is thickened and the muscle appears disorganized, the head is smaller and retinal fusion is delayed (compare distance between small arrows in WT and MO right panels). Scale bar: 500 μm. (**B**) Locomotor activity in the developing zebrafish embryo is disrupted at 20 hpf. Embryo body movement is tracked in a video (Supplementary Material, videos): head movement is tracked in blue and tip of the tail movement in yellow. Both head and tail change position dramatically in the wild type due to spontaneous tail coiling. In the *pomk* morphants, the head and tail always remain in the same relative situation because the embryo is unable to shift position within the chorion. (B) Morphant larvae at 3 dpf show a shorter and bent tail. Scale bar: 500 μm. (**C**) *pomk* morphants muscle at 3 dpf shows signs of muscular dystrophy, laminin and dystrophin (dystr) staining are reduced and glycosylated α-DG is almost completely missing. Disorganization of the muscle fibers can also be noted by the disruption in nuclear orientation revealed by Hoechst staining. Scale bar: 100 μm. (**E**) Injection of human full-length *POMK* mRNA in the *pomk* morphant embryo causes significant phenotypic improvement, while injection of truncated (Q109*) *POMK* mRNA does not (left graph). Overexpression of mRNA up to 1 ng has no effect on the embryos (right graph). Results are from at least three independent experiment and are quantified at 1 dpf scoring the phenotypes shown in Figure 5A. Embryos scored as severe are greatly underdeveloped with barely distinguishable head and tail.

These findings indicate that loss of *pomk* leads to muscular dystrophy in the fish during early embryonic development.

We next asked whether the p.Gln109* mutation identified in the less severe patients acted via a gain- or loss-of-function mechanism. POMK is predicted to be enzymatically inactive and it is possible that it may contribute to assembling a signaling complex with other kinases (18,31). We wondered whether the truncated POMK even without a kinase domain could affect complex formation and act in a dominant negative fashion. We overexpressed up to 1 ng of full-length and truncated (Q109*)

human *POMK* mRNA then scored the embryos for the presence or absence of the phenotypes shown in Figure 5A, but all fish appeared normal up to 3 dpf (Fig. 5E). To show that the mRNA was in fact producing functional protein and to test the effects of the p.Gln109* mutation, we also co-injected the *pomk* splice MO with full-length or truncated human mRNA showing that the full-length human POMK was effective in rescuing the morphant phenotype (*pomk* MO 8.2 ± 2.2% normal embryos; MO + full-length POMK 33.7 ± 2.7% normal embryos; $N = 4$, $P = 0.0003$, Fig. 5E). The truncated mRNA had no effect demonstrating that this mutation most likely leads to a POMK loss of function (Fig. 5E).

DISCUSSION

Phenotypic variability of POMK mutations

Dystroglycanopathies are a group of disorders showing genetic and clinical heterogeneity (1). Mutations in 16 genes have been identified to date to cause phenotypes in the dystroglycanopathy spectrum, but roughly half of the cases still remain unexplained, indicating that even more genetic heterogeneity is to be expected (7,32,33). All 16 known genes are involved in the control of α-DG glycosylation and the regulation of interactions with the ECM, but while six are glycosyltransferases whose substrates are known, the function of many other genes has not been as clearly defined. Genotype–phenotype correlation studies have helped define how each gene is involved in dystroglycan function. Truncating and loss-of-function mutations in the glycosyltransferases *POMT1*, *POMT2*, *B3GALNT2* and *GTDC2* usually cause the most severe dystroglycanopathy, WWS, while hypomorphic missense changes may primarily affect the muscle and cause CMD or LGMD (6,14–17). These enzymes assemble the core M3 glycan which is necessary for α-DG's laminin-binding activity (18) and the extreme severity of these loss-of-function phenotypes of this glycan indicates that this modification may be one of the primary determinants of dystroglycan function.

Our findings define a complex genotype–phenotype correlation for *POMK*, whereby severe truncating mutations can cause both the most severe phenotype in the dystroglycanopathy spectrum, WWS, or one of the least severe, LGMD plus ID. Due to the unavailability of cell lines or tissue from either family, we are unable to test for the presence of residual protein or truncated fragments, yet the combination of an early frameshift (p.Phe96fs) and a missense change (p.Val302Asp) in Family 2 result in a much more severe phenotype than a homozygous nonsense change removing the putative kinase domain (p.Gln109*) in Family 1. The rescue experiments using the mutated *POMK* mRNA following *pomk* knockdown in the zebrafish embryo show that even if a truncated protein is expressed following the p.Gln109* mutation, it is likely to be inactive.

The function of POMK, previously known as Sugen Kinase 196 (SGK196), has only recently been described as a protein involved in the phosphorylation of O-linked mannose (O-Man) in the core M3 glycan and possibly others (18). This phosphorylation event is necessary for the addition to the core M3 glycan of a polysaccharide synthesized by the bifunctional glycosyltransferase LARGE, which is also necessary for laminin binding (13). LARGE assembles a disaccharide chain containing glucuronic acid (GlcA) and xylose (Xyl) in a glycan of variable length (34). The number of disaccharide repeats in these LARGE-glycans has been correlated with muscular disease severity, the extent of muscle fiber regeneration and laminin-binding ability (35). *LARGE* is also mutated in dystroglycanopathies, but there are only a dozen known *LARGE* alleles. Most *LARGE* alleles are copy number variants leading to deletions, duplications or complex rearrangements and there are only two missense and one nonsense alleles. All but one case have severely truncating alleles which cause a spectrum of brain, eye and muscle phenotypes from WWS to CMD with severe cognitive impairment and white matter abnormalities (6,36,37).

The variability in clinical findings between Families 1 and 2 and the variability observed in the additional cases published by other groups (7,19) imply either that the laminin-binding site is variably affected by *POMK* loss of function in different families or that POMK may act in a complex with other proteins, which regulate phosphorylation and allow for normal LARGE-glycan expression. While POMK has been shown to regulate O-Man phosphorylation, sequence analysis indicates that important catalytic residues are missing in this protein, hinting to the possibility that interacting partners may be necessary for its function (18). The phenotypic variability observed in cases with truncating mutations in *LARGE* and *POMK* could also imply an alternative muscle regeneration mechanism independent of both these proteins and more active in some patients than others.

POMK expression and function during early muscle development

No functional data are available for *POMK* loss of function during muscle development. When we explored POMK expression by qPCR analysis in fetal and adult human tissues, we found the highest expression in brain, skeletal muscle, kidney and heart as observed in other dystroglycanopathy genes (16). This is consistent with additional phenotypes often observed in dystroglycanopathies, such as kidney dysplasia, hydronephrosis and cardiomyopathy, which are not part of the core diagnostic features but often accompany brain and muscle findings (1,38). While *POMK* remained highly expressed in brain, heart and kidney in the adult compared with fetal tissues, skeletal muscle expression decreased by >60%. When we analyzed protein expression using immunohistochemistry in fetal and adult skeletal muscle, we observed that POMK is expressed in all cells in the fetal muscle including cells with myogenic potential, but expression decreases in the adult and becomes concentrated in interstitial cells in between the myofibers and within blood vessels. Interstitial cells are a mixed population of unknown function including mesenchymal progenitors and POMK may have different roles in the adult muscle than in the fetal one.

The fetal expression pattern in all myocytes and interstitial cells suggests an important role during muscle development. Mouse models of dystroglycanopathy genes causing severe phenotypes are often early embryonic lethal, but analysis of conditional models removing *Dag1* or *Fktn* at different stages of development have revealed that dystroglycan is important in both early development and regeneration, with worse phenotypes resulting by early developmental defects (39,40).

Because of its fetal distribution, we tested whether loss of *POMK* would result in a defect in early myocyte differentiation and myotube fusion in human myogenic cells purified from fetal muscle samples. While POMK was very strongly expressed throughout myocyte differentiation *in vitro* and knockdown caused a reduction in α-DG glycosylation, we found that myocyte fusion was normal indicating that later stages of differentiation must be affected.

Our studies on the zebrafish provided some insight in the timing of action of *pomk* during development. Differently from the mouse, where dystroglycan glycosylation seems to be more critical for early embryogenesis than in the human, zebrafish phenotypes unfold during embryonic and larval development. Locomotor activity was impaired as early as 20 hpf when the embryos were unable to move freely in the chorion and the brain, eye and muscle appeared affected as 1 dpf. The developing muscle displayed signs of dystrophy and loss of α-DG glycosylation soon after hatching at 3 dpf. Dystrophin and laminin expression at the myosepta were reduced as described in multiple dystroglycanopathy mutants and morphants (16,29,41) and α-DG glycosylation was reduced in the muscle as was observed following POMK knockdown in fetal myocytes.

In conclusion, we identified a role for POMK in early muscle development, likely contributing to the most severe phenotype observed in some patients, but it remains unclear how different truncating mutations may cause variable phenotypes. Additional studies on POMK interacting partners and the identification of more *POMK* alleles are necessary to shed light on the role of this protein.

MATERIALS AND METHODS

Subject enrollment

All subjects were enrolled after informed consent was obtained and research was conducted according to protocols approved by the Institutional Review Board of Boston Children's Hospital. Diagnosis in the dystroglycanopathy spectrum was obtained by assessing a combination of brain, eye and muscle phenotypes that are characteristic of these disorders. A clinical diagnosis of congenital or limb-girdle muscular dystrophy, based on severe hypotonia, elevated serum CK and where possible a histopathological confirmation of muscular dystrophy. At the more severe end of the spectrum the presence of brain malformations including cobblestone lissencephaly, severe ventriculomegaly and brain stem/cerebellar hypoplasia, and of ocular malformations in the retina or anterior chamber of the eye. For less severely affected subjects, a concurrent diagnosis of cognitive impairment or no brain and eye defects was given.

Genome-wide genotyping and exome sequencing

Genomic DNA was prepared from peripheral blood samples or myocytes from patients and available family members according to standard protocols. Six hundred to 1000 ng of genomic DNA was used to hybridize Illumina Human610-Quad single nucleotide polymorphism (SNP) arrays at the Yale Center for Genome Analysis, Yale School of Medicine. Genotyping data were analyzed using the loss of heterozygosity algorithm on dChip software (42) to identify regions of identity by descent. SNP data from each individual were also imported as custom tracks in the UCSC Genome Browser (http://genome.ucsc.edu) for visualization. Ten micrograms of genomic DNA from Patient 1 were used for enrichment via array capture of the three regions of homozygosity identified in this family. Capture arrays were custom designed by Nimblegen and libraries were sequenced on an Illumina 2G machine with coverage of at least 5× for 92% of the target. In all other families, affected individuals were sequenced on an Illumina HiSeq 2000 machine at a coverage averaging at least 50× for 95% of the genome following capture with Agilent SureSelect Human All Exon kits. Sequencing reads were mapped to the reference genome using a custom pipeline and annotated on Annovar software (43). Exome variants from all subjects are combined in a common SQL database where they can be queried. Candidate variants are validated by Sanger sequencing following amplification of the surrounding genomic region by PCR. Sanger sequencing was performed at SeqWright (Houston, TX, USA) or Eurofins (Huntsville, AL, USA). Inheritance pattern was confirmed in all available family members and variant frequency was determined via the Exome Variant Server containing exome data from 6503 samples from the NHLBI Exome Sequencing Project.

SGK196 expression analysis

cDNA samples from human fetal and adult postmortem brain tissue were obtained commercially (BioChain and Clontech). qPCR was performed using SYBR green reagents (SsoFast EvaGreen Supermix from Bio-Rad) on a Bio-Rad platform (CFX384) using the following primers SGK196-For 5′-CTT CTTCATCGCTCCTCGACA-3′ and SGK196-Rev 5′-AGCCA AGGTGAGCAGTTTTTC-3′. Expression was normalized to β-actin (ACTB). Relative expression levels are indicated as ratio to a control sample containing equal amounts of all individual tissue cDNAs.

Cortices were dissected at the indicated embryonic and postnatal days from embryos and pups obtained from wild-type C57BL/6 mice. Lysates were prepared in RIPA buffer (0.5% SDS, 1% Triton X-100, 5 mM EDTA, 2 mM DTT in PBS) plus protease and phosphatase inhibitors (Sigma).

Immunofluorescence staining of muscle tissue sections

Tissue samples from de-identified, discarded human fetal muscle samples at 21 weeks gestational age as well as de-identified, discarded adult autopsy muscle tissue from individuals not affected by muscle disease was frozen in liquid nitrogen chilled isopentane. Tissue was stored at −80 C until further use. These samples were collected under a protocol approved by the Committee of Clinical Investigation at Boston Children's Hospital.

Frozen muscle samples were sectioned on a cryostat at thickness of 7 μm and collected on slides (Tissue Tack Microscope slides; Polysciences). Tissue was fixed with 100% methanol for 3 min followed by several washes in PBS, and 1 h blocking in 10% FBS/PBS, all at room temperature. Sections were incubated with mouse anti-SGK196/POMK (Abcam, ab57908; 1:100), rabbit anti-Laminin (Sigma, 1:500), rabbit anti-LaminA/C (Epitomics, 1:500) in blocking solution o/n at 4°C. The secondary antibodies donkey anti mouse Alexa594 (Invitrogen, 1:500)

and donkey anti rabbit Alexa488 (JacksonImmuno, 1:500) were diluted in PBS and let incubate on sections for 45 min at room temperature. The sections were coverslipped using Vectashield mounting medium with DAPI (Vector Labs).

Cell culture of human fetal myogenic cells

De-identified, discarded human fetal muscle samples were obtained from the Brigham and Women's Hospital, under a protocol approved by Committee of Clinical Investigation. Human fetal myogenic cells were purified by FACS based on expression of MCAM as previously described (24). Myogenic cells were expanded in growth medium consisting of DMEM-high glucose, 20% fetal bovine serum, 100 U/ml penicillin and 100 μg/ml streptomycin. At 65–70% confluence, myogenic cells were induced to differentiate in DMEM-low glucose, 2% horse serum, 100 U/ml penicillin and 100 μg/ml streptomycin. Differentiation medium was changed daily and cells were monitored for myotube formation. Proliferating cells in growth media with high glucose and serum were harvested as Day 0 sample, whereas the differentiating cells were harvested daily and labeled accordingly.

Western blotting

Cell lysates were made with M-PER Mammalian protein extraction reagent (Thermo Scientific) containing protease and phosphatase inhibitor cocktail tablets (Roche Applied Sciences). Twenty-five micrograms of total protein treated with sample loading buffer either with or without β-mercaptoethanol and heated for 10 min at 95°C and separated using Precast NuPage 4–12% Bis–Tris acrylamide gel (Invitrogen) SDS–PAGE. The proteins were wet transferred to nitrocellulose membrane (Bio-Rad). The membranes were blocked with 5% BSA and 1% milk and probed with primary antibodies in the blocking solution, overnight at 4°C. The blots were washed with 1× TBST and labeled with HRP conjugated anti-IgG in 5% milk; then washed again in 1× TBST and developed using ECL solution (Perkin Elmer). The primary antibodies used were anti-SGK196/POMK (Abcam, 1:1000), α-DG (Millipore-1:1000) and β-actin (Sigma 1:5000).

siRNA oligos transfection and analysis

On-Target plus siRNA oligonucleotide pool for human SGK196/POMK was purchased (Thermo Scientific). As controls, On-Target plus control non-target siRNA oligos and On-target plus human GAPDH siRNA duplex (Thermo Scientific) were obtained and reconstituted in the siRNA buffer each at the concentration of 20 μM. siRNA oligos were electroporated in primary $MCAM^+$ myogenic cells with T-012 program using Amaxa NHDF Nucleofector kit (Lonza), as per manufacture's protocol. Optimization and transfection efficiency was determined using the pmax GFP (Lonza). After 48 h, the transfected cells were lysed as mentioned above and used for protein analysis and the rest were stimulated to differentiate and the samples collected in the following consecutive days as described above.

Knockdown of pomk in zebrafish

Fertilized zebrafish oocytes were obtained from Oregon AB breeders maintained by the Aquatic Resources Program at Boston Children's Hospital or by the Manzini lab at the George Washington University as described (44). All animal work was performed in compliance with protocols approved by the Boston Children's Hospital and the George Washington University Animal Care and Use Committees. Microinjection was performed at the one- or two-cell stage (20–45 min postfertilization) using pulled borosilicate pipettes on a PLI-100A Pico-Injector (Harvard Apparatus). Morpholino oligonucleotide (MO) sequences were designed by Gene Tools LLC (Philomat, OR, USA) to target the start site or intron 1 splice donor site of pomk (CR848040.6 bp49392-55962) as follows: sgk196 start CCACCGACAGCAGTGCCACCCATAA and sgk196 splice ACCAATCTCACCAAACTCACCTTCT. Both MOs were injected at 5 ng in 1× Danieau solution (58 mM NaCl, 0.7 mM KCl, 0.4 mM $MgSO_4$, 0.6 mM $Ca(NO_3)_2$, 5 mm HEPES, pH 7.6) with 0.1% phenol red as injection dye. Full-length or truncated (Q109*) POMK mRNA was PCR amplified from an MGC Sequence-Verified cDNA clone obtained from Thermo Scientific (MHS6278-202857477) and cloned into pCS2+ for capped mRNA production. mRNA was produced using the Ambion mMessage mMachine SP6 transcription kit. Embryos were maintained at 28.5°C and staged at hours and days postfertilization.

Zebrafish immunohistochemistry

Embryos and larvae were anesthetized using 0.4% Tricaine stock and fixed in 4% paraformaldehyde in PBS o/n at 4°C. After the fixative was washed away with PBS plus 1% Tween, the samples were equilibrated in 40% sucrose to prepare for cryosection. Samples were then embedded in Neg50 Frozen Section Medium (Thermo Scientific) and 18 μm sections were obtained on a Microm HM-505E cryostat. The strongest immunostaining for laminin and dystrophin was observed in the absence of detergent, so sections were not permeabilized and just blocked in 10% normal goat serum in PBS prior to staining with rabbit anti-laminin (Sigma; 1:75), mouse anti-dystrophin (Sigma; 1:100) or mouse anti-α-DG (clone VIA4-1, Sigma; 1:100). Secondary antibodies were: donkey anti mouse Alexa568 (Life Technologies, 1:500) and donkey anti rabbit Alexa488 (Life Technologies, 1:500). Imaging was performed on a Zeiss Imager M uprights fluorescent microscope.

SUPPLEMENTARY MATERIAL

Supplementary Material is available at *HMG* online.

ACKNOWLEDGEMENTS

First we would like to express our gratitude to the families for their participation in our studies. The EuroBioBank and Telethon Network Genetic Biobanks (GTB07001F) are also acknowledged for providing biological samples. We also thank Chris Lawrence and Jason Best from the Aquatic Research Program at Boston Children's Hospital for help with zebrafish maintenance and injection, Tom Maynard for advice on qPCR assays at the GWU Biomarker Discovery Core, the W.M. Keck Foundation Biotechnology Resource Laboratory

at Yale University for performing genome-wide SNP array hybridization.

Conflict of Interest statement. None declared.

FUNDING

Sequencing at Children's Hospital Boston was supported by the Intellectual and Developmental Disabilities Research Centers (CHB DDRC, P30HD19655). T.W.Y. was supported by an NIH T32 grant (T32NS007484-08), the Clinical Investigator Training Program (CITP) at Harvard-Massachusetts Institute of Technology Health Science and Technology and the Nancy Lurie Marks Junior Faculty MeRIT Fellowship. V.A.G. was supported by an award from the William Randolph Hearst Fund and a K01 award from the NIH (NIAMS, K01AR062601). M.A.S. was supported by the Deanship of Scientific Research, King Saud University, Riyadh, Saudi Arabia through project number RGP-VPP-301. Research was supported by grants from the NIH (NINDS, R01NS035129) to C.A.W. and the Manton Center for Orphan Disease Research to C.A.W. and M.C.M. C.A.W. is an investigator of the Howard Hughes Medical Institute. M.C.M. was also supported by an award from the William Randolph Hearst Fund and a development grant the Muscular Dystrophy Association.

REFERENCES

1. Muntoni, F., Torelli, S., Wells, D.J. and Brown, S.C. (2011) Muscular dystrophies due to glycosylation defects. *Curr. Opin. Neurol.*, **24**, 437–442.
2. Wells, L. (2013) The o-mannosylation pathway: glycosyltransferases and proteins implicated in congenital muscular dystrophy. *J. Biol. Chem.*, **288**, 6930–6935.
3. Cormand, B., Pihko, H., Bayés, M., Valanne, L., Santavuori, P., Talim, B., Gershoni-Baruch, R., Ahmad, A., Van Bokhoven, H., Brunner, H.G. *et al.* (2001) Clinical and genetic distinction between Walker-Warburg syndrome and muscle-eye-brain disease. *Neurology*, **56**, 1059–1069.
4. Dobyns, W.B., Pagon, R.A., Armstrong, D., Curry, C.J., Greenberg, F., Grix, A., Holmes, L.B., Laxova, R., Michels, V.V. and Robinow, M. (1989) Diagnostic criteria for Walker-Warburg syndrome. *Am. J. Med. Genet.*, **32**, 195–210.
5. Balci, B., Uyanik, G., Dincer, P., Gross, C., Willer, T., Talim, B., Haliloglu, G., Kale, G., Hehr, U., Winkler, J. *et al.* (2005) An autosomal recessive limb girdle muscular dystrophy (LGMD2) with mild mental retardation is allelic to Walker-Warburg syndrome (WWS) caused by a mutation in the POMT1 gene. *Neuromuscular Disord.*, **15**, 271–275.
6. Godfrey, C., Clement, E., Mein, R., Brockington, M., Smith, J., Talim, B., Straub, V., Robb, S., Quinlivan, R., Feng, L. *et al.* (2007) Refining genotype phenotype correlations in muscular dystrophies with defective glycosylation of dystroglycan. *Brain*, **130**, 2725–2735.
7. Jae, L.T., Raaben, M., Riemersma, M., van Beusekom, E., Blomen, V.A., Velds, A., Kerkhoven, R.M., Carette, J.E., Topaloglu, H., Meinecke, P. *et al.* (2013) Deciphering the glycosylome of dystroglycanopathies using haploid sScreens for lassa virus entry. *Science*, **340**, 479–483.
8. Barresi, R. and Campbell, K.P. (2006) Dystroglycan: from biosynthesis to pathogenesis of human disease. *J. Cell Sci.*, **119**, 199–207.
9. Pawlisz, A.S. and Feng, Y. (2011) Three-dimensional regulation of radial glial functions by Lis1-Nde1 and dystrophin glycoprotein complexes. *PLoS Biol.*, **9**, e1001172.
10. Moore, S.A., Saito, F., Chen, J., Michele, D.E., Henry, M.D., Messing, A., Cohn, R.D., Ross-Barta, S.E., Westra, S., Williamson, R.A. *et al.* (2002) Deletion of brain dystroglycan recapitulates aspects of congenital muscular dystrophy. *Nature*, **418**, 422–425.
11. Stalnaker, S.H., Hashmi, S., Lim, J.-M., Aoki, K., Porterfield, M., Gutierrez-Sanchez, G., Wheeler, J., Ervasti, J.M., Bergmann, C., Tiemeyer, M. *et al.* (2010) Site mapping and characterization of O-glycan structures on alpha-dystroglycan isolated from rabbit skeletal muscle. *J. Biol. Chem.*, **285**, 24882–24891.
12. Nilsson, J., Nilsson, J., Larson, G. and Grahn, A. (2010) Characterization of site-specific O-glycan structures within the mucin-like domain of alpha-dystroglycan from human skeletal muscle. *Glycobiology*, **20**, 1160–1169.
13. Yoshida-Moriguchi, T., Yu, L., Stalnaker, S.H., Davis, S., Kunz, S., Madson, M., Oldstone, M.B.A., Schachter, H., Wells, L. and Campbell, K.P. (2010) O-mannosyl phosphorylation of alpha-dystroglycan is required for laminin binding. *Science*, **327**, 88–92.
14. Van Reeuwijk, J., Janssen, M., van den Elzen, C., Beltran-Valero de Bernabé, D., Sabatelli, P., Merlini, L., Boon, M., Scheffer, H., Brockington, M., Muntoni, F. *et al.* (2005) POMT2 mutations cause alpha-dystroglycan hypoglycosylation and Walker-Warburg syndrome. *J. Med. Genet.*, **42**, 907–912.
15. Beltrán-Valero De Bernabé, D., Currier, S., Steinbrecher, A., Celli, J., van Beusekom, E., van der Zwaag, B., Kayserili, H., Merlini, L., Chitayat, D., Dobyns, W.B. *et al.* (2002) Mutations in the O-mannosyltransferase gene POMT1 give rise to the severe neuronal migration disorder Walker-Warburg syndrome. *Am. J. Hum. Genet.*, **71**, 1033–1043.
16. Manzini, M.C., Tambunan, D.E., Hill, R.S., Yu, T.W., Maynard, T.M., Heinzen, E.L., Shianna, K.V., Stevens, C.R., Partlow, J.N., Barry, B.J. *et al.* (2012) Exome sequencing and functional validation in zebrafish identify GTDC2 mutations as a cause of Walker-Warburg syndrome. *Am. J. Hum. Genet.*, **91**, 541–547.
17. Stevens, E., Carss, K.J., Cirak, S., Foley, A.R., Torelli, S., Willer, T., Tambunan, D.E., Yau, S., Brodd, L., Sewry, C.A. *et al.* (2013) Mutations in B3GALNT2 cause congenital muscular dystrophy and hypoglycosylation of α-dystroglycan. *Am. J. Hum. Genet.*, **92**, 354–365.
18. Yoshida-Moriguchi, T., Willer, T., Anderson, M.E., Venzke, D., Whyte, T., Muntoni, F., Lee, H., Nelson, S.F., Yu, L. and Campbell, K.P. (2013) SGK196 is a glycosylation-specific O-Mannose kinase required for dystroglycan function. *Science*, **341**, 896–899.
19. von Renesse, A., Petkova, M.V., Lützkendorf, S., Heinemeyer, J., Gill, E., Hübner, C., von Moers, A., Stenzel, W. and Schuelke, M. (2014) POMK mutation in a family with congenital muscular dystrophy with merosin deficiency, hypomyelination, mild hearing deficit and intellectual disability. *J. Med. Genet.*, **51**, 275–282.
20. Martínez-Lage, J.F., Pérez-Espejo, M.A., Almagro, M.-J. and López-Guerrero, A.L. (2011) Hydrocephalus and arachnoid cysts. *Childs Nerv. Syst.*, **27**, 1643–1652.
21. Lander, E. and Botstein, D. (1987) Homozygosity mapping: a way to map human recessive traits with the DNA of inbred children. *Science*, **236**, 1567–1570.
22. Yu, T.W., Chahrour, M.H., Coulter, M.E., Jiralerspong, S., Okamura-Ikeda, K., Ataman, B., Schmitz-Abe, K., Harmin, D.A., Adli, M., Malik, A.N. *et al.* (2013) Using whole-exome sequencing to identify inherited causes of autism. *Neuron*, **77**, 259–273.
23. Cullen, M., Elzarrad, M.K., Seaman, S., Zudaire, E., Stevens, J., Yang, M.Y., Li, X., Chaudhary, A., Xu, L., Hilton, M.B. *et al.* (2011) GPR124, an orphan G protein-coupled receptor, is required for CNS-specific vascularization and establishment of the blood-brain barrier. *Proc. Natl. Acad. Sci. USA*, **108**, 5759–5764.
24. Anderson, K.D., Pan, L., Yang, X.-M., Hughes, V.C., Walls, J.R., Dominguez, M.G., Simmons, M.V., Burfeind, P., Xue, Y., Wei, Y. *et al.* (2011) Angiogenic sprouting into neural tissue requires Gpr124, an orphan G protein-coupled receptor. *Proc. Natl. Acad. Sci. USA*, **108**, 2807–2812.
25. Lapan, A.D., Rozkalne, A. and Gussoni, E. (2012) Human fetal skeletal muscle contains a myogenic side population that expresses the melanoma cell-adhesion molecule. *Hum. Mol. Genet.*, **21**, 3668–3680.
26. Lapan, A.D. and Gussoni, E. (2012) Isolation and characterization of human fetal myoblasts. *Methods Mol. Biol.*, **798**, 3–19.
27. Gibbs, E.M., Horstick, E.J. and Dowling, J.J. (2013) Swimming into prominence: the zebrafish as a valuable tool for studying human myopathies and muscular dystrophies. *FEBS J.*, **280**, 4187–4197.
28. Saint-Amant, L. and Drapeau, P. (1998) Time course of the development of motor behaviors in the zebrafish embryo. *J. Neurobiol.*, **37**, 622–632.
29. Gupta, V., Kawahara, G., Gundry, S.R., Chen, A.T., Lencer, W.I., Zhou, Y., Zon, L.I., Kunkel, L.M. and Beggs, A.H. (2011) The zebrafish dag1 mutant: A novel genetic model for dystroglycanopathies. *Hum. Mol. Genet.*, 10.1093/hmg/ddr047.

30. Lin, Y.-Y., White, R.J., Torelli, S., Cirak, S., Muntoni, F. and Stemple, D.L. (2011) Zebrafish Fukutin family proteins link the unfolded protein response with dystroglycanopathies. *Hum. Mol. Genet.*, **20**, 1712–1725.
31. Manning, G., Whyte, D.B., Martinez, R., Hunter, T. and Sudarsanam, S. (2002) The protein kinase complement of the human genome. *Science*, **298**, 1912–1934.
32. Manzini, M.C., Gleason, D., Chang, B.S., Hill, R.S., Barry, B.J., Partlow, J.N., Poduri, A., Currier, S., Galvin-Parton, P., Shapiro, L.R. *et al.* (2008) Ethnically diverse causes of Walker-Warburg syndrome (WWS): FCMD mutations are a more common cause of WWS outside of the Middle East. *Hum. Mutat.*, **29**, E231–E241.
33. Roscioli, T., Kamsteeg, E.-J., Buysse, K., Maystadt, I., Van Reeuwijk, J., Van Den Elzen, C., van Beusekom, E., Riemersma, M., Pfundt, R., Vissers, L.E.L.M. *et al.* (2012) Mutations in ISPD cause Walker-Warburg syndrome and defective glycosylation of [alpha]-dystroglycan. *Nat. Genet.*, **44**, 581–585.
34. Inamori, K.-I., Yoshida-Moriguchi, T., Hara, Y., Anderson, M.E., Yu, L. and Campbell, K.P. (2012) Dystroglycan function requires xylosyl- and glucuronyltransferase activities of LARGE. *Science*, **335**, 93–96.
35. Goddeeris, M.M., Wu, B., Venzke, D., Yoshida-Moriguchi, T., Saito, F., Matsumura, K., Moore, S.A. and Campbell, K.P. (2013) LARGE glycans on dystroglycan function as a tunable matrix scaffold to prevent dystrophy. *Nature*, **503**, 136–140.
36. Longman, C., Brockington, M., Torelli, S., Jimenez-Mallebrera, C., Kennedy, C., Khalil, N., Feng, L., Saran, R.K., Voit, T., Merlini, L. *et al.* (2003) Mutations in the human LARGE gene cause MDC1D, a novel form of congenital muscular dystrophy with severe mental retardation and abnormal glycosylation of alpha-dystroglycan. *Hum. Mol. Genet.*, **12**, 2853–2861.
37. Clarke, N.F., Maugenre, S., Vandebrouck, A., Urtizberea, J.A., Willer, T., Peat, R.A., Gray, F., Bouchet, C., Manya, H., Vuillaumier-Barrot, S. *et al.* (2011) Congenital muscular dystrophy type 1D (MDC1D) due to a large intragenic insertion/deletion, involving intron 10 of the LARGE gene. *Eur. J. Hum. Genet.*, **19**, 452–457.
38. Devisme, L., Bouchet, C., Gonzales, M., Alanio, E., Bazin, A., Bessières, B., Bigi, N., Blanchet, P., Bonneau, D., Bonnières, M. *et al.* (2012) Cobblestone lissencephaly: neuropathological subtypes and correlations with genes of dystroglycanopathies. *Brain*, **135**, 469–482.
39. Beedle, A.M., Nienaber, P.M. and Campbell, K.P. (2007) Fukutin-related protein associates with the sarcolemmal dystrophin-glycoprotein complex. *J. Biol. Chem.*, **282**, 16713–16717.
40. Cohn, R.D., Henry, M.D., Michele, D.E., Barresi, R., Saito, F., Moore, S.A., Flanagan, J.D., Skwarchuk, M.W., Robbins, M.E., Mendell, J.R. *et al.* (2002) Disruption of DAG1 in differentiated skeletal muscle reveals a role for dystroglycan in muscle regeneration. *Cell*, **110**, 639–648.
41. Kawahara, G., Guyon, J.R., Nakamura, Y. and Kunkel, L.M. (2010) Zebrafish models for human FKRP muscular dystrophies. *Hum. Mol. Genet.*, **19**, 623–633.
42. Leykin, I., Hao, K., Cheng, J., Meyer, N., Pollak, M.R., Smith, R.J.H., Wong, W.H., Rosenow, C. and Li, C. (2005) Comparative linkage analysis and visualization of high-density oligonucleotide SNP array data. *BMC Genet.*, **6**, 7.
43. Wang, K., Li, M. and Hakonarson, H. (2010) ANNOVAR: functional annotation of genetic variants from high-throughput sequencing data. *Nucleic Acids Res.*, **38**, e164.
44. Lawrence, C. (2011) Advances in zebrafish husbandry and management. *Methods Cell Biol.*, **104**, 429–451.